Flux-closure chirality control and domain wall trapping in asymmetric magnetic ring

Cite as: J. Appl. Phys. **106**, 043905 (2009); https://doi.org/10.1063/1.3197413
Submitted: 01 January 2009 . Accepted: 13 July 2009 . Published Online: 21 August 2009

X. H. Wang, W. K. Peng, and W. S. Lew

Flux-closure chirality control and domain wall trapping in asymmetric magnetic ring

X. H. Wang, W. K. Peng, and W. S. Lew[a)]
Physics and Applied Physics Division, School of Physical and Mathematical Sciences, Nanyang Technological University, 21 Nanyang Link, Singapore 637371, Singapore

(Received 1 January 2009; accepted 13 July 2009; published online 21 August 2009)

A technique for flux-closure chirality control and domain wall trapping at the narrowest position in asymmetric magnetic ring is proposed. Micromagnetic simulation work was performed on permalloy asymmetric magnetic rings to observe its magnetic switching behavior. By controlling the lateral geometric features, the ring asymmetry, and the thickness of the film, a local vortex-free reversal process and well-controlled chirality of flux closure can be achieved. Furthermore, a domain wall trapping feature is also observed at the narrow arm of the asymmetric ring, which corresponds to the phenomenon that the magnetic domain wall does not annihilate until the magnetization in the wide arm reversed in a relatively large magnetic field. A phase diagram of the asymmetric ring switching behavior shows that the switching regimes (e.g., the domain wall propagation or nucleation annihilation) of the asymmetric rings and the domain wall pinning depend mainly on the film thickness. © *2009 American Institute of Physics*. [DOI: 10.1063/1.3197413]

I. INTRODUCTION

Small magnetic elements have been extensively studied over the years because of its promising applications ranging from the data storage, magnetic logic gate to sensing device. With the advent of modern nanofabrication and characterization techniques, we are able to observe the magnetic properties of these magnetic elements down to the nanoscale regime, which was once a major challenge to uncover the mystery of the fundamental physics involving the study of the equilibrium magnetic states and magnetization reversal mechanisms. Extensive research has been carried out on square or rectangular[1,2] structures as well as highly symmetric structures such as disk[3] and ring[4–6] structures. Nanoscale ring structures are of particular interest due to the removal of its perpendicularly magnetized vortex core; two magnetic states have been observed in studies of nanoscale ring structures known as the flux-closure state[7] and the bidomain state (or "onion" state). In the remnant flux-closure state, external magnetic field is not generated, thus the cross interaction between neighboring elements can be suppressed. This could give the advantage for the magnetic elements being used in magnetic memory devices.

Recently much interest has been given to the flux-closure state in which the magnetization is oriented circumferentially and domain wall does not present. This state has been proposed for magnetic storage devices and layered structure of the magnetoresistive random access memory (MRAM) in which the magnetization rotation is exploited to store one data bit.[8] In order to control the magnetization rotation direction, which is essential for wide range of applications, much effort had been devoted to the investigation of the chirality of the vortex under the influence of the in-plane magnetic field as well as polarized current. The chirality has been manipulated by using a flat edge in disks,[9] notches in rings,[10] and disks with off-centered core.[11,12] In this work, we present a study on the nanoscale ring structure with inner circle off-centered and for various thicknesses by means of micromagnetic simulations. Our results show that through deliberate controlling of the parameters of the asymmetric rings, local vortex core-free switching process can be obtained and the control of chirality of the flux closure can be realized by exploiting the asymmetric feature in the nanoring. When the thickness of the asymmetric ring is smaller than 12 nm, a pair of head-to-head and tail-to-tail domain walls[13] can be trapped at the thinner arm of the asymmetric ring in a wide range of lateral size ranging from several hundred nanometers to submicron. The domain wall trapping feature is not only relevant for potential application such as controlling fast switching in magnetic random access memory cells but also to be utilized in magnetotransport studies.[14] Based on this simulation results, we propose a method to control the domain wall position in the nanoscale ring without having to deliberately create notches.[13]

II. SIMULATION

The magnetization configuration and switching properties were simulated using the object oriented micromagnetic framework (OOMMF) simulation program.[15] In this simulation, the micromagnetic equilibrium equations were solved in a two dimensional square mesh with a cell size of 4 nm and the spins are free to rotate in three dimensions. A ramping magnetic field from −1500 to 1500 G in the asymmetrical axis of asymmetric ring (AC in Fig. 1) in 60 steps was applied. Other parameters used for the permalloy were crystalline anisotropy constant $K_1=0$, saturation magnetization $M_s=8.6\times10^5$ A m^{-1}, exchange stiffness $A=1.3\times10^{-11}$ J m^{-1}, and the damping coefficient $\alpha=0.5$. The asymmetric ratio R of the ring is defined as $R=l/(D_o-D_i)$, where l is the displacement distance of the internal circle from the outer circle, while D_o and D_i are the outer and inner

a)Electronic mail: wensiang@ntu.edu.sg.

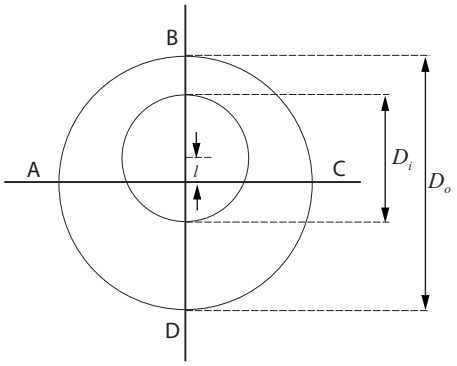

FIG. 1. Geometry of the asymmetric magnetic ring used in the simulation. An example of asymmetric magnetic ring for ratio $R=0.2$ is shown here. For clarity, we refer to the asymmetric axis as AC and the symmetric axis as BD.

diameters of the ring, respectively, as depicted in Fig. 1. For the initial part of this work, D_o and D_i as well as the thickness t were varied at fixed $R=0.2$ to observe their effects on the switching mechanisms and behavior. Subsequently, calculations on asymmetric ring for $R=0.1$ and $R=0.3$ were also presented for comparison.

III. RESULTS AND DISCUSSIONS

In order to study the effect of the lateral size and thickness of the asymmetric magnetic ring on the switching processes and mechanisms, a wide range of outer diameter of the ring ($D_o=400$, 600, 800, 1000, 1200, and 1400 nm) and the film thickness ($t=8$, 12, 16, 20, 24, 28, and 32 nm) were performed. The effect of the D_i, which bears some similarity to the influence of ring width as in the case of the symmetric ring, is also studied: for a fixed $D_o=1200$ nm and for various inner diameter ($D_i=600$, 800, and 900 nm). Our calculations revealed that when the inner circle is off-centered by a ratio $R=0.2$, a triple-switch loop with two plateaus can be seen. This is in contrast to the double switching that occurs in symmetric ring structures reported by van Belle *et al.*[16] The simulated hysteresis loop indicates a number of magnetization states along with different magnetic field strengths applied: negative saturation, bidomain, vortex, reverse bidomain, and positive saturation. Typically simulated hysteresis loop of the asymmetric ring (for a fixed $D_o=1200$ nm and $D_i=600$ nm) for $t=12$ nm, $t=8$ nm is shown in Figs. 2(a) and 2(b), respectively. Insets show its corresponding magnetic configurations. In Fig. 2(a) the first two switches in the loop are due to the propagation of the domain walls via the thinner and the thicker arms of the asymmetric ring. The third switch is caused by the domain wall annihilation in the wider arm of the asymmetric ring. The annihilation of the domain wall in the wider arm causes a magnetization drop, which is similar as the symmetric ring as reported by Klaui *et al.*[17] This resemblance in hysteresis loop is due to the similarity of the geometric feature since the wider arm of the asymmetric ring can be seen as a part of a wide symmetric ring. However switching behaviors of asymmetric ring with $t=8$ nm are quite different: instead of forming a flux closure after the bidomain state, the two domain walls in the thin arm do not annihilate and a pair of head-to-head and tail-to-tail domain walls is trapped at the narrowest point of the

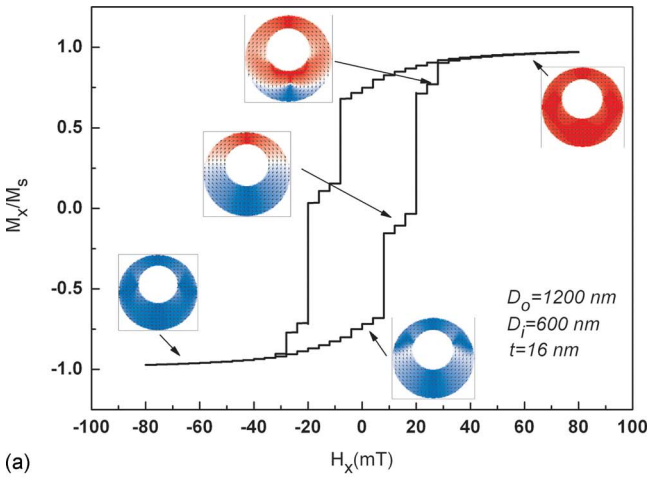

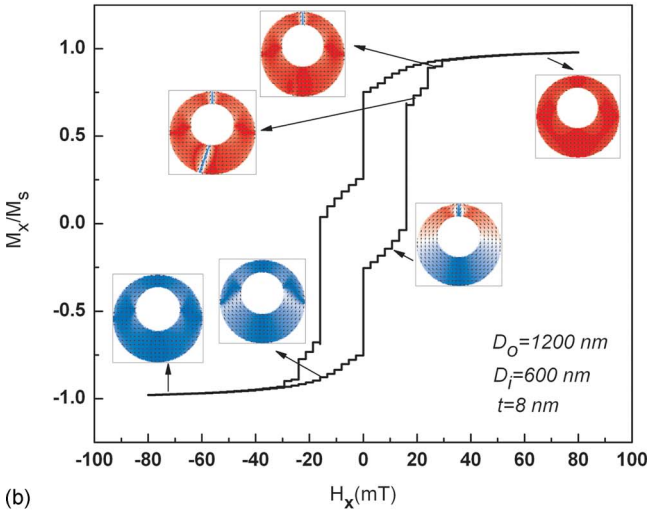

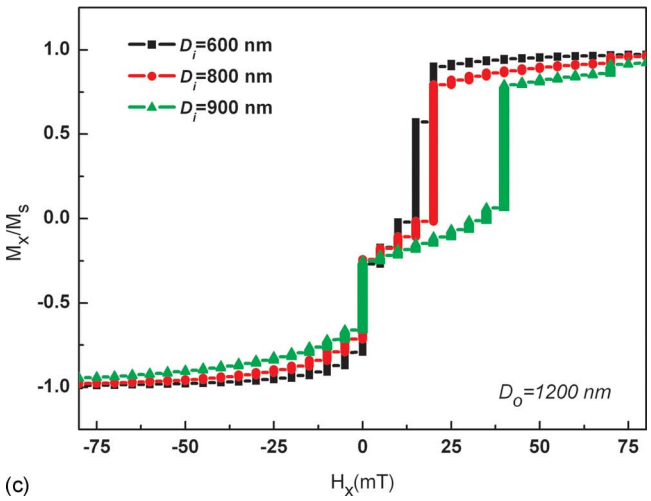

FIG. 2. (Color online) Typically simulated hysteresis loops of asymmetric magnetic ring for $D_o=1200$ nm, (a) $t=16$ nm, and (b) $t=8$ nm and its magnetic configurations (shown in insets). (c) Hysteresis loop of the asymmetric magnetic ring for various $D_i=600$, 800, and 900 nm at a fixed $D_o=1200$ nm and $t=8$ nm.

ring. When the reversed magnetic field is large enough, the trapped domain wall annihilates. Figure 2(b) shows the switching process. The hysteresis loop is similar to that in asymmetric ring with a thickness of 16 nm, except that there is one additional small plateau. This small plateau is caused

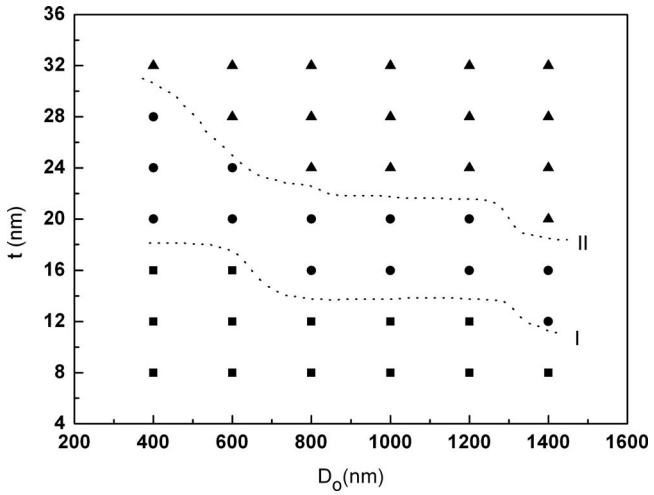

FIG. 3. Phase diagram of switching as a function of the ring geometrical parameters, i.e., the thickness of the film and the outer diameter of the ring for $D_i/D_o=0.5$; line I and line II are two boundaries separating following three kinds of switching: (i) transverse domain wall propagation in the thin arm (■), (ii) vortex nucleation in the wide arm (●), and (iii) multinucleation switching (▲).

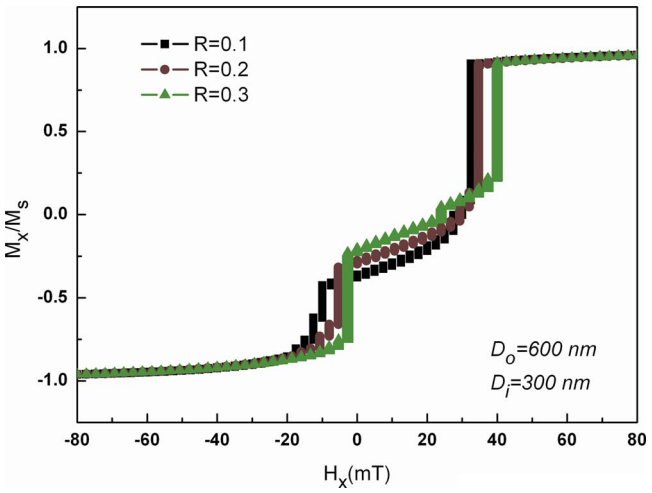

FIG. 4. (Color online) Simulated hysteresis loops of the asymmetric magnetic ring for various asymmetric ratio of $R=0.1$, 0.2, and 0.3. Other geometrical parameters of the asymmetric rings were arbitrarily chosen as $D_o=600$ nm, $D_i=300$ nm, and $t=16$ nm.

by the trapped domain wall. The annihilation of this trapped domain corresponds to the last switch in the hysteresis loop. We further varied the inner diameter from 600 to 800 and 900 nm of the asymmetric ring for the same $t=8$ nm and calculated the magnetic switching process. The switching processes are similar to the process shown in Fig. 2(b). Figure 2(c) is the calculated hysteresis loop of asymmetric ring with inner diameters of 600, 800, and 900 nm. From the hysteresis loop we can see that the switching field increases as the ring arm width decreases, which is probably due to the uneven edge acting as pinning sites for the domain walls.

From the switching process of the asymmetric ring, the circulation of the flux-closure state determined by the spin direction in the wider arm of the asymmetric ring can be seen. Since the narrowest point of the asymmetric ring is the energy minimum position for the transverse walls, the domain walls nucleated at the asymmetric axis (AC in Fig. 1) at large field will selectively move to the position of lower energy, which is the narrowest point of the ring arm (B in Fig. 1). By this selectivity of the domain wall movement, the circulation of the flux-closure state can be controlled by applying a magnetic field along the symmetric axis direction of the asymmetric ring. An elegant way of controlling the circulation of flux closure was proposed by Vavassori *et al.*[11] by introducing a void in a disk. Compared to their methods, our flux-closure control using asymmetric ring can attain a local vortex-free switching process by using different inner diameters and asymmetric ratios.

In order to investigate the influence of geometric parameters such as ring width, thickness, and outer diameter to the switching process, we systematically studied the switching processes and the switching field distributions. Figure 3 shows the phase diagrams of the asymmetric ring switching behavior. In the phase diagram there are two significant boundaries. The first boundary is at line I. Below line I, a pair of head-to-head and tail-to-tail domain walls can be trapped at the thinner arm of the asymmetric ring. This trapped domain wall does not annihilate until a relatively large magnetic field is applied, as shown previously for asymmetric ring of a $D_o=1200$ nm (Fig. 2). The annihilation of the trapped domain wall causes the last small switch in the hysteresis loop. The second boundary is at line II. This line separates the switching process of the simple domain wall propagation reversal and multinucleation and annihilation reversal. Above line II, the switching process is via multinucleation and annihilation. In between line I and line II, the switching process is simple domain wall propagation which corresponds to the squares in Fig. 3. This result shows that the film thickness is the key factor that determines the switching behavior and separating the three switching regimes.

We further varied the distances between the inner and outer circles of the asymmetric rings to investigate the influence of asymmetric ratio on the switching behavior. The lateral sizes of the asymmetric rings used here are $D_o=600$ nm, $D_i=300$ nm. The thickness of the rings is 16 nm. The asymmetric ratios used were $R=0.1$, 0.2, and 0.3 which means that the distances between the center of the inner and outer circles were 30, 60, and 90 nm, respectively. According to our calculations, with same lateral size and thickness, the switching behaviors of asymmetric rings with asymmetric ratios $R=0.1$, 0.2, and 0.3 are quite similar, as shown in the insets of Fig. 2. The most significant influence of the asymmetric ratio is that with a larger asymmetric ratio, the field to drive the domain walls nucleated at the symmetric axis of the asymmetric ring becomes smaller (Fig. 4), which means the domain walls in the asymmetric ring move easier. This easier movement of the domain wall corresponds to the earlier switch in the loop when applying the same magnetic field. With increment of asymmetric ratio, the sensitivity of the domain wall to the magnetic field increases. The influence of magnetic field on the domain wall has the same trend as what was reported elsewhere.[17]

For a thin film magnetic nanoring, the magnetization lies in the plane of the film because of the shape anisotropy. The

total energy is thus the sum of the exchange and the magnetostatic terms[18] and the spin configurations are determined by the minimization of the sum of the energy terms. For the asymmetric rings in this work, the energy minimum position for annihilated transverse domain walls will be at point B in Fig. 1. To explain the circulation control and energy minimum position of the asymmetric ring, we use the model proposed by Tchernyshyov and Chern.[19] The domain walls can be seen as composite objects made of two or more elementary defects and are held together by competition between attractive Coulomb force and the confinement of the edge. In an asymmetric ring within the thin film limit ($\lambda^2\rangle\rangle wt$, where λ is the magnetic length, w is the ring width, and t is the thickness), the domain wall energy can be evaluated as[12] $E \approx 2\pi A \log(ewt \log(w/t)/\pi\lambda^2)$, where A is the exchange stiffness. When the asymmetric ring is thick and wide in the magnetostatic regime ($\lambda^2\langle\langle wt$), which is similar to our simulation case, the magnetostatic energy is minimized only when the bulk density of magnetic charges vanishes. On the surface, the configuration[19] of the domain wall is that the two defects at the inner circle remain as in the thin film limit, while at the outer circle the two defects emanate in opposite directions and form a V shaped domain wall, which is similar to the two domain walls annihilated in the asymmetric axis of the asymmetric ring. The domain wall energy in this regime is still an increasing function of w and t. Therefore when the initial field along ac is decreasing, two transverse domain walls will be generated at ac with a large energy slope. In near remanence, the two domain walls will tend to slide toward the energy minimum position B to lower the energy of the whole system. The effect of anisotropy energy can be neglected since it plays no significant role as compared to the magnetostatic term. As the magnetic field increases, the Zeeman energy will dominate instead of the magnetostatic energy, which explains why the domain wall propagates across the wider arm of the asymmetric ring and the wall annihilates.

IV. CONCLUSION

A technique to trap a domain wall at the exact position in asymmetric magnetic ring is proposed. By controlling the geometry of the nonmagnetic ring, simple and reproducible switching can be obtained. The switching field dependency of permalloy asymmetric magnetic rings was studied by means of micromagnetic simulations. When the thickness is controlled to a range, a pair of head-to-head and tail-to-tail domain walls can be trapped at the thinner arm of the asymmetric ring. The vortex circulation can be also controlled using asymmetry. The phase diagram of the switching behavior through the asymmetric rings of different regimes and domain wall trapping is presented as a function of ring thickness, inner diameter and outer diameter. It is found that the boundary between different switching regimes depends much more on the thickness than the other two geometric parameters. The sensitivity of the domain wall nucleated at the symmetric axis of the asymmetric ring is reducing with decreasing of the asymmetric ratio. The experimental work is under progress and will be reported elsewhere.

ACKNOWLEDGMENTS

This work is supported by the ASTAR SERC grant (Contract No. 0821010015) and the National Research Foundation (CRP project: Multifunctional Spintronic Materials and Devices).

[1] K. J. Kirk, J. N. Chapman, S. McVitie, P. R. Aitchison, and C. D. W. Wilkinson, Appl. Phys. Lett. **75**, 3683 (1999).
[2] J. Yu and U. Rudiger, J. Appl. Phys. **85**, 5501 (1999).
[3] T. Taniuchi, M. Oshima, H. Akinaga, and K. Ono, J. Electron Spectrosc. Relat. Phenom. **144-147**, 741 (2005).
[4] M. Kläui, C. A. F. Vaz, L. Lopez-Diaz, and J. A. C. Bland, J. Phys.: Condens. Matter **15**, R985 (2003).
[5] C. A. Ross, F. J. Castano, D. Morecroft, W. Jung, H. I. Smith, T. A. Moore, T. J. Hayward, J. A. C. Bland, T. J. Bromwich, and A. K. Petford-Long, J. Appl. Phys. **99**, 08S501 (2006).
[6] Y. G. Yoo, M. Klaui, C. A. F. Vaz, L. J. Heyderman, and J. A. C. Bland, Appl. Phys. Lett. **82**, 2470 (2003).
[7] X. Y. Kong, Y. Ding, R. Yang, and Z. L. Wang, Science **303**, 1348 (2004).
[8] J.-G. Zhu, Y. Zheng, and G. A. Prinz, J. Appl. Phys. **87**, 6668 (2000).
[9] R. Nakatani, T. Yoshida, Y. Endo, Y. Kawamura, M. Yamamoto, T. Takenaga, S. Aya, T. Kuroiwa, S. Beysen, and H. Kobayashi, J. Appl. Phys. **95**, 6714 (2004).
[10] M. Klaui, J. Rothman, L. Lopez-Diaz, C. A. F. Vaz, J. A. C. Bland, and Z. Cui, Appl. Phys. Lett. **78**, 3268 (2001).
[11] P. Vavassori, R. Bovolenta, V. Metlushko, and B. Ilic, J. Appl. Phys. **99**, 053902 (2006).
[12] F. Q. Zhu, G. W. Chern, O. Tchernyshyov, X. C. Zhu, J. G. Zhu, and C. L. Chien, Phys. Rev. Lett. **96**, 027205 (2006).
[13] M. Klaui, J. Phys.: Condens. Matter **20**, 313001 (2008).
[14] O. Boulle, J. Kimling, P. Warnicke, M. Klaui, U. Rudiger, G. Malinowski, H. J. M. Swagten, B. Koopmans, C. Ulysse, and G. Faini, Phys. Rev. Lett. **101**, 216601 (2008).
[15] The OOMMF package is available at http://math.nist.gov/oommf.
[16] F. van Belle, T. J. Hayward, J. A. C. Bland, and W. S. Lew, J. Appl. Phys. **102**, 103908 (2007).
[17] M. Klaui, C. A. F. Vaz, J. A. C. Bland, E. Sinnecker, A. P. Guimaraes, W. Wernsdorfer, G. Faini, E. Cambril, L. J. Heyderman, and C. David, Appl. Phys. Lett. **84**, 951 (2004).
[18] C. A. F. Vaz, T. J. Hayward, J. Llandro, F. Schackert, D. Morecroft, J. A. C. Bland, M. Klaui, M. Laufenberg, D. Backes, U. Rudiger, F. J. Castano, C. A. Ross, L. J. Heyderman, F. Nolting, A. Locatelli, G. Faini, S. Cherifi, and W. Wernsdorfer, J. Phys.: Condens. Matter **19**, 255207 (2007).
[19] O. Tchernyshyov and G. W. Chern, Phys. Rev. Lett. **95**, 197204 (2005).